International Conference on Textile Composites and Inflatable Structures
STRUCTURAL MEMBRANES 2011
E. Oñate, B. Kröplin and K.-U.Bletzinger (Eds)

SHEAR AND BENDING STIFFNESSES OF ORTHOTROPIC INFLATABLE TUBES

J.-C. THOMAS*

* GeM, Institute for Research in Civil and Mechanical Engineering, CNRS UMR 6183
LUNAM University, University of Nantes-Centrale Nantes
2, rue de la Houssiniere BP 92208 44322 Nantes Cedex 3, France
e-mail: jean-christophe.thomas@univ-nantes.fr

Key words: Bending and shear stiffnesses, Inflatable Beam, Orthotropic Fabrics

Abstract. This work concerns the behavior of inflatable beams subjected to bending loads. Some authors have worked on this subject and strength of materials theories have been written. In this paper, we first propose to calculate precisely the radius and length of inflated tubes which are needed to use the strength of materials theory in the case of high pressure. The usual linear equations are not precise enough and it is needed to use a non-linear set of equations. The second part focuses on the strength of materials theory. The assumptions that the straight section remains in a plane after deformation is first considered. Then the shear and bending stiffnesses are identified by the use of the results of a $3D$ code dedicated to inflatable structures which takes into account the orthotropic behavior of fabrics. Finally, a correction of the moduli is proposed. This correction takes into account the variation of geometry between the natural state, which corresponds to the non inflated beam, and the initial state which corresponds to the inflated beam.

1 INTRODUCTION

Inflatable objects are widely used nowadays to built temporary structures. They are often made of assemblies of elementary parts like panels, tubes, arches or cones. These elements can be calculated with a strength of materials theory. In the case of inflatable structures, three states can be taken into account. The first state is the "natural" state. In this case, there is no pressure in the structure and the fabric has geometrical dimensions that change when the structure is pressurized. After inflation, a new state called "initial" state is reached. It corresponds to the structure when it is just subjected to the internal pressure. The "final" state is obtained when other external loadings are applied. Strength of materials theory is commonly used to predict the behavior of the structure between the initial and the final state. It has been written mainly in the case of tubes, panels and cones. This work concerns the behavior of inflatable tubes and it is important to

quantify correctly the geometrical dimensions of the structures at the initial state. The modern fabrics used on earth are more resistant, and therefore it is possible to consider important pressures inside the beams. In these cases, the linear equations that have been written using the assumptions of little deformations to estimate the length and the radius of inflated tubes just after the first inflation are less precise. This demands then to study the evolution of the radius and the length as function of the pressure in the case of important deformations. This will lead to a non-linear set of equations. Once the radius and the length of the tube are known, it is possible to use strength of materials theory. Bernoulli's kinematic has been used in some papers[1],[2],[3],[4] . Some authors have written strength of materials theories based on Timoshenko's assumptions in the case of inflatable structures [5],[6],[7],[8]. The second part of the paper concerns the behavior of tubes submitted to bending loads. First of all, the behavior of the straight section is quantified in order to verify the validity of the assumption that the straight section remains in a plane or not. Afterwards, the paper is focused on the shear and the bending rigidities in the case of orthotropic tubes. The bending and the shear rigidities of inflatable tubes can be obtained following different formulations[7],[8]. The results are similar because the bending stiffnesses are the same and the shear stiffnesses present a little difference. The use of the results of a $3D$ code will allow to see which theoretical formulation is the closer to the $3D$ results. The last part concerns the moduli of the fabrics taken into account in strength of materials theory. In fact, the evolutions of the bending and shear stiffnesses as function of the pressure show that it is important to take into account the changing of observer between the natural and the initial state.

2 RADIUS AND LENGTH IN THE CASE OF HIGH PRESSURE

2.1 The different states

In the case of inflatable structures, two steps of loading are necessary as can be seen on Figure 1 . The starting point is called natural state. It corresponds to the geometrical definition of the fabric without any pressure inside the beam. Index $\oslash$ corresponds to the natural state. $\ell_\oslash$ is the natural length of the beam and $r_\oslash$ is its natural radius. During the inflation, some tension is inducted in the walls and the beam is rigidified. This first step of loading ends with the definition of the geometry of the beam called initial or reference state. The index 0 corresponds to the reference state. So, just after inflation, the characteristic dimensions become the initial length ℓ_0 and the initial radius r_0. The final state (named also current state) of the beam is attended after the second step which corresponds to the application of external loads.

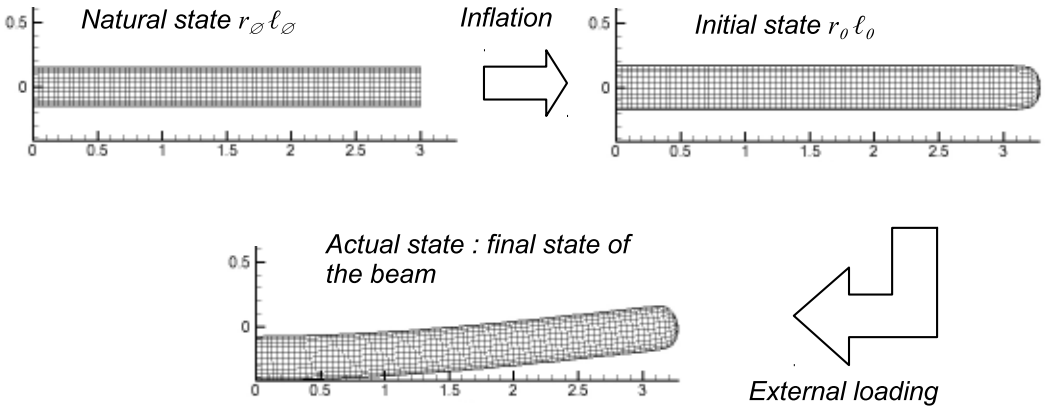

Figure 1: Steps of inflation

2.2 Linear equations used to calculate the radius and the length of inflatable tubes

In some papers, the two dimensions ℓ_0 and r_0 are calculated with the linear formulations obtained from the longitudinal and normal stresses in an inflated tube and by using the Saint Venant Kirchoff behavior law in the case of an orthotropic fabric. This is written with the small deformation assumptions.
Let denote X and Y a local basis where X corresponds to the longitudinal direction of the beam. In this work, the warp direction lines up the longitudinal direction of the beam. X is then parallel to the warp direction of the fabric, and Y is parallel to the weft direction. E_ℓ is the Young modulus in the warp direction, E_t is the Young modulus in the weft direction. $\nu_{t\ell}$ and $\nu_{\ell t}$ are the Poisson's ratio.
In the case of the inflation of a tube, the stress and the strain tensors follow the behavior law:

$$\left\{ \begin{array}{c} \sigma_{XX} \\ \sigma_{YY} \end{array} \right\} = \left[\begin{array}{cc} \overline{E_\ell} & \nu_{t\ell}\overline{E_\ell} \\ \nu_{\ell t}\overline{E_t} & \overline{E_t} \end{array} \right] \left\{ \begin{array}{c} \varepsilon_{XX} \\ \varepsilon_{YY} \end{array} \right\} \tag{1}$$

where $\overline{E_\ell} = \frac{E_\ell}{1-\nu_{\ell t}\nu_{t\ell}}$ and $\overline{E_t} = \frac{E_t}{1-\nu_{\ell t}\nu_{t\ell}}$. In the case of an inflated beam, we assume that the Cauchy strains are :

- longitudinal stress: $\sigma_\ell = \frac{pR_0}{2}$.
- transversal stress: $\sigma_t = pR_0$

and the longitudinal and transversal strains are uniform: $\varepsilon_{XX} = \frac{\Delta\ell_\varnothing}{\ell_\varnothing} = \frac{\ell_0-\ell_\varnothing}{\ell_\varnothing}$ and $\varepsilon_{YY} = \frac{\Delta R_\varnothing}{R_\varnothing} = \frac{R_0-R_\varnothing}{R_\varnothing}$
The use of the behavior law and of the longitudinal and transversal stresses allows us to obtain the following set of equations:

$$\left\{ \begin{array}{l} \frac{pR_\varnothing}{2} = \overline{E_\ell}\varepsilon_{XX} + \nu_{t\ell}\overline{E_\ell}\varepsilon_{YY} \\ pR_\varnothing = \nu_{\ell t}\overline{E_t}\varepsilon_{XX} + \overline{E_t}\varepsilon_{YY} \end{array} \right. \tag{2}$$

We finally obtain:

$$\ell_0 = \ell_\oslash + \frac{pR_\oslash \ell_\oslash}{2E_\ell}(1 - 2\nu_{lt}) \tag{3a}$$

$$R_0 = R_\oslash + \frac{pR_\oslash^2}{2E_t}(2 - \nu_{lt}) \tag{3b}$$

2.3 Non linear set of equations used to calculate the radius and length of the initial state

If high pressure are used, the linear results are less close to the results of the $3D$ code, and it is therefore required to use a Lagrangian formulation. In the case of the inflation of a tube, the Piola Kirchof stress tensor and the Green Lagrange strain tensor follow the behavior law:

$$\left\{ \begin{array}{c} \Sigma^{XX} \\ \Sigma^{YY} \end{array} \right\} = \left[\begin{array}{cc} \overline{E_\ell} & \nu_{t\ell}\overline{E_\ell} \\ \nu_{\ell t}\overline{E_t} & \overline{E_t} \end{array} \right] \left\{ \begin{array}{c} E_{XX} \\ E_{YY} \end{array} \right\} \tag{4}$$

where $\overline{E_\ell} = \frac{E_\ell}{1-\nu_{\ell t}\nu_{t\ell}}$ and $\overline{E_t} = \frac{E_t}{1-\nu_{\ell t}\nu_{t\ell}}$.

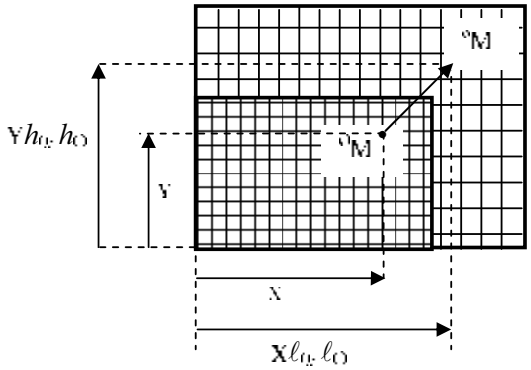

Figure 2: Steps of inflation

Figure 2 presents a piece of fabric subjected to two tensions and the displacement of a point between the natural and the initial states. $\ell_\oslash$ is the length of the rectangular piece of fabric in the natural state and $h_\oslash$ is its width. If X and Y are the coordinates of a point M in the natural state ($^\oslash M$), then $X\frac{\ell_0}{\ell_\oslash}$ and $Y\frac{h_0}{h_\oslash}$ are the coordinates of the point M in the initial state (^0M). The displacements of the points are:

$$\left\{ \begin{array}{l} u_X(X,Y) = X\frac{\ell_0 - \ell_\oslash}{\ell_\oslash} \\ u_Y(X,Y) = Y\frac{h_0 - h_\oslash}{h_\oslash} \end{array} \right. \tag{5}$$

Concerning the radius, we assume that $\frac{h_0}{h_\oslash} = \frac{2\pi r_0}{2\pi r_\oslash} = \frac{r_0}{r_\oslash}$. It allows to calculate the displacement gradient tensor and deduce the deformation gradient tensor:

$$\overline{\overline{F}} = \left[\begin{array}{cc} \frac{\ell_0}{\ell_\oslash} & 0 \\ 0 & \frac{r_0}{r_\oslash}0 \end{array} \right] \tag{6}$$

and the jacobian is $J = \frac{r_0 \ell_0}{r_\oslash \ell_\oslash}$. The Cauchy stresses are $\sigma_\ell = \frac{pR_0}{2}$ and $\sigma_t = pR_0$.

The second Piola-Kirchoff stress tensor is calculated with: $\overline{\overline{\Sigma}} = J\overline{\overline{F}}^{-1}\overline{\overline{\sigma}}\overline{\overline{F}}^{-T}$, consequently:

$$\overline{\overline{\Sigma}} = \begin{bmatrix} \frac{pR_0}{2}\frac{\ell_\oslash h_0}{\ell_0 h_\oslash} & 0 \\ 0 & pR_0\frac{h_\oslash \ell_0}{h_0 \ell_\oslash} \end{bmatrix} \tag{7}$$

The Lagrangian finite strain tensor becomes:

$$\overline{\overline{E}} = \begin{bmatrix} \frac{1}{2}\left(\left(\frac{\ell_0}{\ell_\oslash}\right)^2 - 1\right) & 0 \\ 0 & \frac{1}{2}\left(\left(\frac{R_0}{R_\oslash}\right)^2 - 1\right) \end{bmatrix} \tag{8}$$

following the behavior law, and using the relation $\nu_{t\ell}E_\ell = \nu_{\ell t}E_t$, it is possible to write

$$\begin{cases} \Sigma^{XX} - \nu_{\ell t}\Sigma^{YY} = E_\ell E_{XX} \\ \Sigma^{YY} - \nu_{t\ell}\Sigma^{XX} = E_t E_{YY} \end{cases} \tag{9}$$

We get then the following set of equations:

$$\begin{cases} \frac{pR_\oslash}{2}\frac{\ell_\oslash}{\ell_0}\left(\frac{R_0}{R_\oslash}\right)^2 - \nu_{\ell t}pR_\oslash\frac{\ell_0}{\ell_\oslash} = \overline{E_\ell}\frac{1}{2}\left(\left(\frac{\ell_0}{\ell_\oslash}\right)^2 - 1\right) \\ pR_\oslash\frac{\ell_0}{\ell_\oslash} - \nu_{t\ell}\frac{p}{2}\frac{\ell_0}{\ell_\oslash}\left(\frac{R_0}{R_\oslash}\right)^2 = \overline{E_t}\frac{1}{2}\left(\left(\frac{R_0}{R_\oslash}\right)^2 - 1\right) \end{cases} \tag{10}$$

If one writes $\widetilde{X} = \frac{\ell_0}{\ell_\oslash}$ and $\widetilde{Y} = \frac{R_0}{R_\oslash}$, the system can be re-written under the following form:

$$\begin{cases} \widetilde{X}^3 + \frac{2\nu_{\ell t}pR_\oslash}{E_\ell}\widetilde{X}^2 - \frac{pR_\oslash}{E_\ell}\widetilde{Y}^2 - \widetilde{X} = 0 \\ \widetilde{Y}^2\widetilde{X} - \frac{2pR_\oslash}{E_t}\widetilde{X}^2 + \frac{p\nu_{t\ell}R_\oslash}{E_t}\widetilde{Y}^2 - \widetilde{X} = 0 \end{cases} \tag{11}$$

This finally leads to a non-linear set of equations which can be easily solved.

2.4 Comparisons with the results of the $3D$ code

The theoretical radius and length are compared to the results of a $3D$ code. This finite element code is a non-linear program dedicated to the study of membrane structures based on the total Lagrangian formulation. The membrane elements have zero bending stiffness and satisfy the plane stress conditions. They are supposed to have an orthotropic behaviour. Locally, the warp and weft direction allow to define a basis, which is called orthotropic basis. In this local orthotropic basis, the relation between the 2nd Piola - Kirchhoff stress tensor and the Green Lagrange strain tensor is written by using the following parameters: E_ℓ, the Young's modulus in the warp direction, E_t, the Young's modulus in the weft direction, $G_{\ell t}$ the in-plane shear modulus, and $\nu_{\ell t}$ and $\nu_{t\ell}$ are the

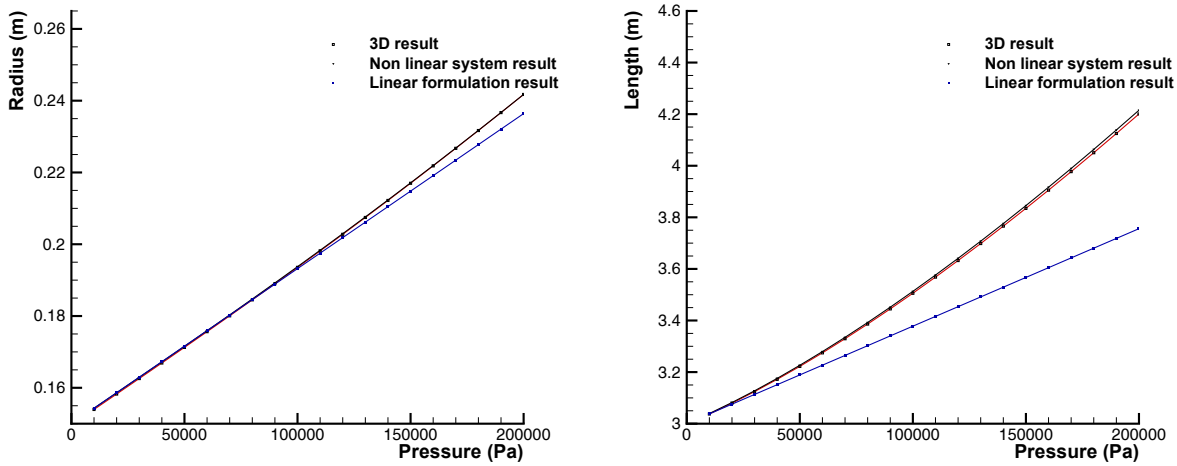

Figure 3: Radius and length of an inflated tube

Poisson's ratios that respect the following equality: $\frac{\nu_{\ell t}}{E_\ell} = \frac{\nu_{t\ell}}{E_t}$.

$$\left\{ \begin{array}{c} \overline{\Sigma}^{11} \\ \overline{\Sigma}^{22} \\ \overline{\Sigma}^{12} \end{array} \right\} = \left[\begin{array}{ccc} \frac{E_\ell}{1-\nu_{\ell t}\nu_{t\ell}} & \frac{\nu_{t\ell}E_\ell}{1-\nu_{\ell t}\nu_{t\ell}} & 0 \\ \frac{\nu_{\ell t}E_t}{1-\nu_{\ell t}\nu_{t\ell}} & \frac{E_t}{1-\nu_{\ell t}\nu_{t\ell}} & 0 \\ 0 & 0 & G_{\ell t} \end{array} \right] \left\{ \begin{array}{c} \overline{E}_{11} \\ \overline{E}_{22} \\ 2\overline{E}_{12} \end{array} \right\} \tag{12}$$

The graphics on Figure 3 present the results of the inflation of an inflatable beam. The moduli of the fabrics used here are products of the moduli by the thickness. Therefore, the surface of the straight section is replaced by $S = 2\pi r$ and the second bending momentum is replaced by $I = \pi r^3$. The moduli are $E_\ell = E_t = 50000\ MPa.m$, $G_{\ell t} = 12500\ MPa.m$, $\nu_{\ell t} = 0.08$. The non linear set of equations has been solved here by using the solver of Microsoft Excel. It shows that if the pressure is important the length and the radius are not linear function of the pressure. This is most important in the case of the length. The use of the linear formulation can lead to quite important relative errors. In the case studied here, the relative error for the length is greater than 10%. It is in the range of 2% in the case of the radius. The results of the non-linear set of equations is much closer to the results of the $3D$ code than the results of the linear formulation, and justify the use of the non linear approach in such cases.

3 BEHAVIOR OF THE STRAIGHT SECTION

Following Timoshenko's assumptions, the straight section is supposed to remain in a plane but not orthogonal to the neutral fibber. Since this phenomenon is all the more important that the beam supports heavy loads, the choice has been done to consider the

case of a clamped-simply supported beam subjected to a local load in the middle of the beam. The radius of the beam considered here is 0.3 m and its length is 6 m. The moduli of the fabric are $E_\ell = E_t = 160000 Pa.m$, $G_{\ell t} = 16000 Pa.m$ and $\nu_{\ell t} = 0.08$. The inside pressure is 2000 Pa and the applied load is 800 N. In this case, the displacement of the point in the middle of the beam is 0.167 m. The left figure of Figure 4 shows the planes orthogonal to the neutral fibber and the trace of the projection of the points of a straight section in a deformed position. The right figure shows the distances of every points of the straight section to the medium plane of the points of the straight section. Following Saint-Venant principle, the sections considered here are not too close to the points of loading. The assumptions that inflatable tubes follow a Timoshenko's kinematic is then valuable. The Figure 5 presents the evolution of $\frac{dv}{dx} - \theta$ along the beam obtained with the $3D$ code.

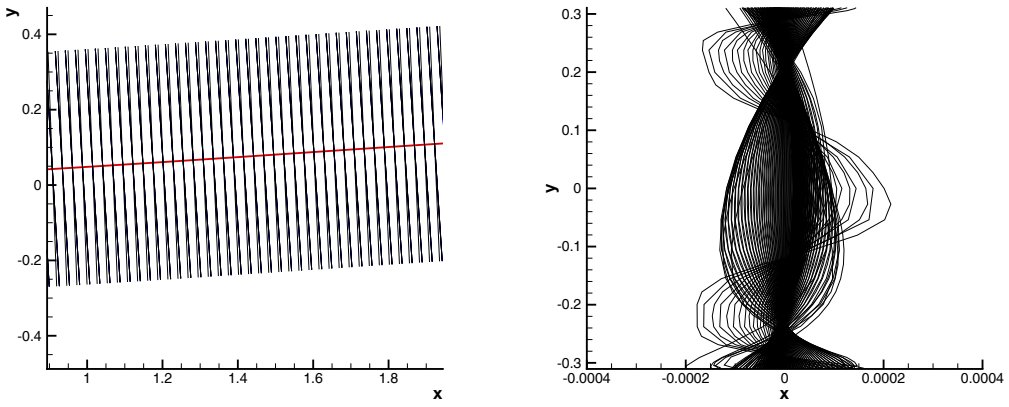

Figure 4: Behavior of the straight section of an inflated beam

.

4 BENDING STIFFNESS AND SHEAR STIFFNESS

4.1 Analytical stiffnesses of a cantilever inflated beam

Two formulations have recently been written to calculate the deflection of inflatable beams. The first one has been written in the case of inflatable tubes made of isotropic

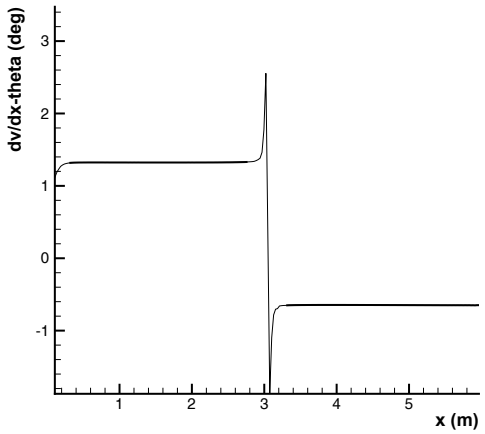

Figure 5: $\frac{dv}{dx} - \theta$ obtained with the $3D$ code

material[7]. In this case, the deflection of the beam is:

$$v(x) = \frac{F}{(E + P/S_0)I_0}\left(\frac{x^3}{6} - \frac{\ell_0 x^2}{2}\right) - \frac{Fx}{P + kGS_0} \tag{13a}$$

$$\theta(x) = \frac{F}{(E + P/S_0)I_0}\left(\frac{x^2}{2} - \ell_0 x\right) \tag{13b}$$

where E is the Young elasticity modulus and G is the shear elasticity modulus.

The case of orthotropic fabrics has also been written [8]. In the case of a cantilever inflated beam, the results are:

$$v(x) = \frac{F}{(E_{or} + P/S_0)I_0}\left(\frac{x^3}{6} - \frac{\ell_0 x^2}{2}\right) - \frac{Fx}{P + \frac{1}{2}kG_{or}S_0} \tag{14a}$$

$$\theta(x) = \frac{F}{(E_{or} + P/S_0)I_0}\left(\frac{x^2}{2} - \ell_0 x\right) \tag{14b}$$

where $E_{or} = \dfrac{E_\ell}{1 - \nu_{\ell t}\nu_{t\ell}}$ and $G_{or} = G_{\ell t}$. By replacing E by E_{or} and G by G_{or} in the isotropic formulation, it is possible to obtain another formulation to calculate the deflection of the beam in the orthotropic case. The bending parts of the deflection are the same but there exists a difference in the shear part due to a coefficient $1/2$. The results of the $3D$ code will be compared to the different analytical results.

4.2 Identification of the stiffnesses

The shear and the bending stiffnesses are identified by using the Timoshenko's strength of materials theory. In the case of a cantilever beam, the equilibrium equations and the

boundary conditions lead to:

$$kGS(\frac{dv}{dx} - \theta) = F \qquad and \qquad EI\frac{d^2\theta}{dx^2} = -F \tag{15}$$

Let's denote R_B the bending rigidity and R_s the shear rigidity.

$$R_s = \frac{F}{\frac{dv}{dx} - \theta} \qquad and \qquad R_B = -\frac{F}{\frac{d^2\theta}{dx^2}} \tag{16}$$

The quantities $\frac{dv}{dx} - \theta$ and $\frac{d^2\theta}{dx^2}$ are determined with the $3D$ membrane code in the case of a cantilever inflatable beam.

4.3 Comparison between the analytical stiffnesses and the results of the $3D$ code

Figures 6 and 7 present the results of the comparison between the theoretical stiffnesses and the identified stiffnesses. It is clear that they are non linear function of the pressure. In the case of the Figure 6, the moduli are $E_\ell = E_t = 50000\ MPa.m$, $G_{\ell t} = 12500\ MPa.m$, $\nu_{\ell t} = 0.08$. The curve $EI + PI/S$ is close to the curve of the $3D$ results for little pressures, but it differs for higher pressures. In the case of the shear rigidity, $P + kGS$ is coincident with the $3D$ results in the case of little pressures and $P + 1/2kGS$ is inferior. For higher pressures, the both curves differ to the $3D$ results. The Figure 7 presents analogous results. In this case, the moduli are $E_\ell = E_t = 50000\ MPa.m$, $G_{\ell t} = 12500\ MPa.m$, $\nu_{\ell t} = 0.3$ This has been done to look at the influence of the Poisson's ratio. The same conclusions can be written.

The divergence between the curves decreases by using a correction of the moduli of the fabrics used in the analytical formulations. The strength of materials theory allows to study the behavior of the bended beam between the initial and the final states. The comparisons are made by using the moduli that have been used with the $3D$ code. These moduli are used in reference to the natural state. The fact that the strength of materials concerns the behavior of the beam between the initial and final states, and not between the natural and final states which is the case of the $3D$ numerical developpements, demands to take into account the changing of geometry between the two states.
This can be done by using the Piola Kirchoff stress tensor and the Green Lagrange strains tensor and changing the observer between the natural state and the initial state. The use of the behavior law leads finally to the definition of ${}^{\oslash}E_\ell$ and ${}^{0}E_\ell$. ${}^{\oslash}E_\ell$ is the Young modulus in the warp direction used in the $3D$ simulations. It corresponds to the fabric in the natural state. ${}^{0}E_\ell$ is the Young modulus in the warp direction used in the strength of materials theory. It corresponds to the fabric in the initial state. These corrective coefficients are geometrical terms which come from the variation of geometry due to the pressurization. For example, in the case of the Young modulus, the correction is:${}^{0}E_\ell = \frac{h_\oslash}{h_0}\left(\frac{\ell_0}{\ell_\oslash}\right)^3 {}^{\oslash}E_\ell$.

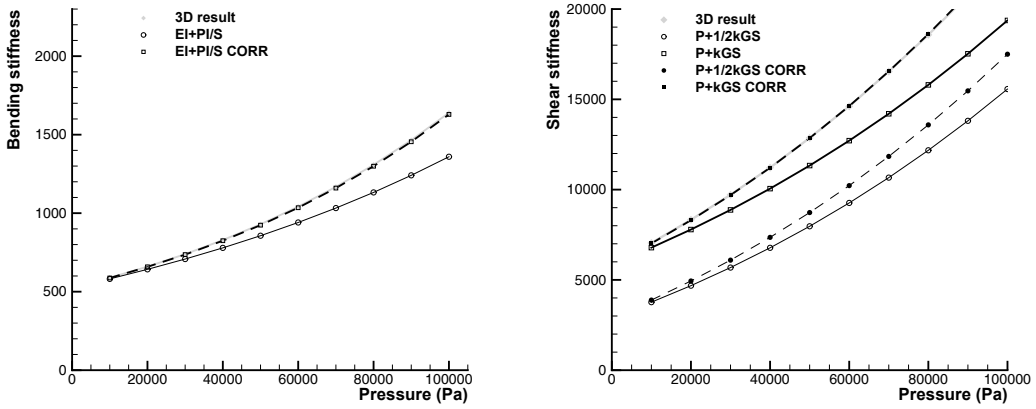

Figure 6: Theoretical and numerical bending and shear stiffnesses - first fabric

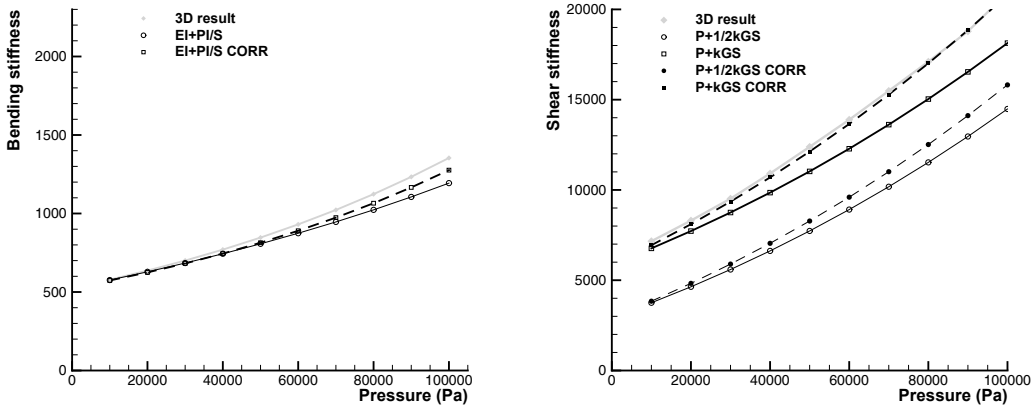

Figure 7: Theoretical and numerical bending and shear stiffnesses - second fabric

The results of the corrections of the moduli can be seen on Figures 6 and 7. The curves $EI + PI/S\ CORR$ and $P + kGS\ CORR$ show the effect of the use of the corrective coefficients on the theoretical stiffnesses. In the case of $\nu_{\ell t} = 0.08$, the shear and bending analytical stiffnesses are coincident to the results of the $3D$ code. In the case of $\nu_{\ell t} = 0.3$, the curve $P + kGS\ CORR$ lines up with the shear rigidity obtained with the numerical simulation. In the case of the bending stiffness, the use of the corrective coefficient leads to an improvement of the analytical result.

5 CONCLUSIONS

The use of high pressure in inflatable structures require to make clearly the difference between the natural state of the beam and the initial state. This is due to the fact that the initial state is the reference in the case of the use of a strength of materials theory. In this work, the geometrical dimensions of the pressurized beam are established by using a non-linear set of equations. Then the assumptions that the straight section remains in a plane is verified. The bending and shear stiffnesses of different theories are compared to the results of a $3D$ code dedicated to inflatable structures. Finally, geometrical coefficients allow to correct the theoretical stiffnesses.

REFERENCES

[1] R.L. Comer and S. Levy, "Deflections of an inflated circular cylindrical cantilever beam", *AIAA Journal 1*, **7**, 1652–1655 (1963).

[2] J.A. Main, S.W. Peterson and A.M. Strauss, "Load-deflection behaviour of space-based inflatable fabric beams", *J. Aerospace. Eng. 2*, **7**, 225-238 (1994).

[3] J. P. H. Webber, "Deflections of inflated cylindrival cantilever beams subjected to bending and torsion", *Aeronautical Journal*, 306–312 (1982).

[4] J.A. Main, R.A. Carlin, E. Garcia, S.W. Peterson and A.M. Strauss, "Dynamic analysis of space-based inflated beam structures", *J. Acoustic. Soc. Am.*, 97, 1035-1042 (1995)

[5] WB. Fichter "A theory for inflated thin-wall cylindrical beams", *NASA TN* D-3466 (1966).

[6] J.-C Thomas and C. Wielgosz, "Deflections of highly inflated fabric tubes", *Thin-Walled Structures*, **42**, 1049-1066 (2004).

[7] A. Levan and C. Wielgosz, "Bending and buckling of inflatable beams: some new theoretical results",*Thin-Walled Structures*;**43**, 116687 (2005).

[8] K.L. Apedo, S. Ronel, E. Jacquelin, M. Massenzio and A. Bennani, "Theoretical analysis of inflatable beams made from orthotropic fabric", *Thin-Walled Structures*, **47**, 1507–1522 (2009).